

Temporal Analysis of Measured LOS Massive MIMO Channels with Mobility

Paul Harris*, Steffen Malkowsky[†], Joao Vieira[†], Fredrik Tufvesson[†], Wael Boukley Hasan*, Liang Liu[†]
Mark Beach*, Simon Armour* and Ove Edfors[†]

*CSN Group, University of Bristol, U.K.

Email: {paul.harris, wb14488, m.a.beach, simon.armour}@bristol.ac.uk

[†]Dept. of Electrical and Information Technology, Lund University, Sweden

Email: firstname.lastname@eit.lth.se

Abstract—The first measured results for massive multiple-input, multiple-output (MIMO) performance in a line-of-sight (LOS) scenario with moderate mobility are presented, with 8 users served by a 100 antenna base Station (BS) at 3.7 GHz. When such a large number of channels dynamically change, the inherent propagation and processing delay has a critical relationship with the rate of change, as the use of outdated channel information can result in severe detection and precoding inaccuracies. For the downlink (DL) in particular, a time division duplex (TDD) configuration synonymous with massive MIMO deployments could mean only the uplink (UL) is usable in extreme cases. Therefore, it is of great interest to investigate the impact of mobility on massive MIMO performance and consider ways to combat the potential limitations. In a mobile scenario with moving cars and pedestrians, the correlation of the MIMO channel vector over time is inspected for vehicles moving up to 29 km/h. For a 100 antenna system, it is found that the channel state information (CSI) update rate requirement may increase by 7 times when compared to an 8 antenna system, whilst the power control update rate could be decreased by at least 5 times relative to a single antenna system.

Index Terms—Massive MIMO, 5G, Testbed, Field Trial, Mobility

I. INTRODUCTION

Massive multiple-input, multiple-output (MIMO) has established itself as a key 5G technology that could drastically enhance the capacity of sub-6 GHz communications in future wireless networks. By taking the multi-user (MU) MIMO concept and introducing additional degrees of freedom in the spatial domain, the multiplexing performance and reliability of such systems can be greatly enhanced, allowing many tens of users to be served more effectively in the same time-frequency resource [1]. In addition to theoretical work and results such as those documented in [1], [2], [3] and [4], various institutions from around the world have been developing large-scale test systems in order to validate theory and test algorithms with real data. Some known examples include the Rice University Argos system [5] [6], the Ngarra demonstrator in Australia [7], the Full Dimension MIMO (FD-MIMO) work by Samsung [8] [9], field trials by ZTE [10] and Project Aries by Facebook [11]. The work presented here is underpinned by 100-antenna and 128-antenna real-time testbeds developed by Lund University and the University of Bristol in collaboration with National Instruments [12] [13]. In 2016, two indoor trials were

conducted within an atrium at the University of Bristol, and it was shown that spectral efficiencies of 79.4 bits/s/Hz and subsequently 145.6 bits/s/Hz could be achieved whilst serving up to 22 user clients [14] [15]. These spectral efficiency results are currently world records and indicate the potential massive MIMO has as a technology.

However, wireless technology is usually applied in scenarios that will involve some form of mobility, and it is therefore of great interest to investigate the evolution of massive MIMO channels under more dynamic conditions. The aforementioned measurement trials have not yet considered the progression of a composite massive MIMO channel with mobility, but measured static terminals. In [16], the authors discuss some of the potential issues with channel ageing in a macro-cell massive MIMO deployment and propose a novel ultra-dense network (UDN) approach for comparison. From simulation results, they illustrate that massive MIMO performance could significantly worsen with mobile speeds of just 10 km/h, and that the sensitivity of zero-forcing (ZF) to channel state information (CSI) errors could make matched filtering (MF) the more viable option. In [17] and [18], the theoretical impact of channel ageing on the uplink (UL) and downlink (DL) performance of massive MIMO is evaluated. Interestingly, the analysis shows that a large number of antennas is to be preferred for maximum performance, even under time-varying conditions, and that Doppler effects dominate over phase noise.

In this paper, 8 user equipments (UEs) are served by a 100 antenna base Station (BS) in real-time and the correlation over time for both the power and MIMO channel is measured for speeds of up to 29 km/h. To the best of the authors' knowledge, these are the first measured results for massive MIMO under moderate mobility in line-of-sight (LOS).

II. SYSTEM DESCRIPTION

The Lund University massive MIMO BS pictured in Fig. 1 consists of 50 National Instruments (NI) universal software radio peripherals (USRPs), which are dual-channel software-defined radios (SDRs) with reconfigurable field-programmable gate arrays (FPGAs) connected to the radio frequency (RF) front ends [19]. Collectively, these provide 100 RF chains, with a further 6 USRPs acting as 12 single-antenna UEs. It

TABLE I
SYSTEM PARAMETERS

Parameter	Value
# of BS Antennas	100
# of UEs	12
Carrier Frequency	1.2-6 GHz (3.7 GHz used)
Bandwidth	20 MHz
Sampling Frequency	30.72 MS/s
Subcarrier Spacing	15 kHz
# of Subcarriers	2048
# of Occupied Subcarriers	1200
Frame duration	10 ms
Subframe duration	1 ms
Slot duration	0.5 ms
TDD periodicity	1 slot

runs with a time division duplex (TDD) LTE-like physical layer (PHY) and the key system parameters can be seen in Table I. Using the same peripheral component interconnect express (PCIe) eXtensions for instrumentation (PXIe) platform that powers the 128-antenna system, all the remote radio heads (RRHs) and MIMO FPGA co-processors are linked together by a dense network of gen 3 PCIe fabric, and all software and FPGA behaviour is programmed via LabVIEW. A description of the Lund University system along with a general discussion of massive MIMO implementation issues can be found in [13]. The reciprocity calibration approach designed at Lund University and applied in these experiments is detailed in [20]. Further detail about the current system architecture and the implementation of a wide data-path Minimum Mean Square Error (MMSE) encoder/decoder can be found in [14], [15] and [21].

A. Antenna Array

The Lund antenna array in Fig. 1 consists of half-wavelength spaced 3.7 GHz patch-antennas each with horizontal and vertical polarization options. For the results reported here, the 4x25 azimuth dominated portion highlighted in the image was used, with alternating horizontal and vertical polarizations across the array.

B. Channel Acquisition

The system is defined as having M antennas, K users and N frequency domain resource blocks of size R_b . For this paper, we specifically define resource block to refer to a grouping of 12 Orthogonal Frequency Division Multiplexing (OFDM) subcarriers, with each 1200 subcarrier OFDM symbol consisting of 100 resource blocks. The estimate of the UL for each 12 subcarrier resource block r is found as

$$\mathbf{H}_r = \mathbf{Y}_r \mathbf{P}_r^* \quad (1)$$

where \mathbf{H}_r is the $M \times K$ channel matrix, \mathbf{Y}_r is the $M \times R_b$ receive matrix and \mathbf{P}_r^* is the diagonal $R_b \times K$ conjugate uplink pilot matrix. Each UE sends an UL pilot for each resource



Fig. 1. Lund Massive MIMO Basestation with 4x25 array configuration highlighted

block on a subcarrier orthogonal to all other users and the BS performs least-square channel estimation. Since all pilots have a power of 1, $\mathbf{Y}_r \mathbf{P}_r^*$ can be used rather than $\mathbf{Y}_r / \mathbf{P}_r^*$. All MIMO processing in the system is distributed across 4 Kintex 7 FPGA co-processors, each processing 300 of the 1200 subcarriers. In order to study the channel dynamics under increased levels of mobility, a high time resolution is desired during the capture process, which equates to a high rate of data to write to disk. To address this, a streaming process was implemented that uses the on-board dynamic random access memory (DRAM) to buffer the raw UL subcarriers. \mathbf{Y}_r is recorded in real-time to the DRAM at the measurement rate, $T_{\text{meas}} = 5$ ms, and this data is then siphoned off to disk at a slower rate. Using this process with 2 GB of DRAM per MIMO processor, we were able to capture the full composite channel for all resource blocks a 5 ms resolution for 65 s.

The channel was sampled at least once every half-wavelength distance in space to give an accurate representation of the environment. The maximum permissible speed of mobility, v_{max} , is thus given by

$$v_{\text{max}} = \frac{\lambda}{2T_{\text{meas}}}. \quad (2)$$

This results in a maximum speed of 8.1 m/s or approximately 29 km/h for temporal analysis of the channel data in this case.

C. Post-Processing

To evaluate the change in the multi-antenna channels under mobility, an analog of the time correlation function (TCF)

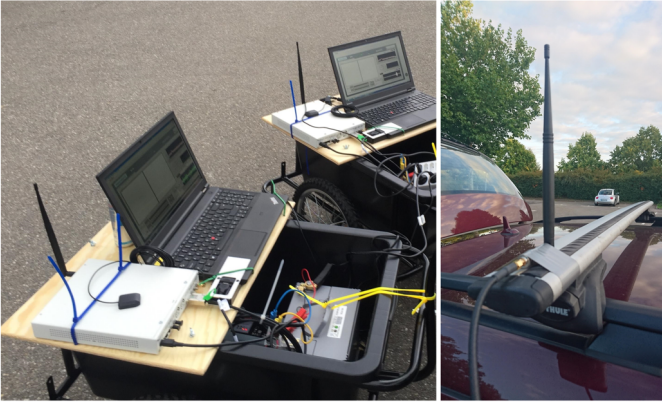


Fig. 2. User Equipments. Left: pedestrian carts. Right: car mounting.

[22] was calculated. By introducing a time dependence on the measured channels, i.e., the channel vector corresponding to user i at resource block r and at time t is denoted by $\mathbf{h}_{i,r}[t]$, the TCF was defined as

$$\text{TCF}_i(\tau) = \frac{\mathbf{E}\{|\mathbf{h}_{i,r}[t-\tau]^H \mathbf{h}_{i,r}[t]|\}}{\mathbf{E}\{\mathbf{h}_{i,r}[t]^H \mathbf{h}_{i,r}[t]\}}, \quad (3)$$

where $\mathbf{E}\{\}$ denotes the expectation operator. At a given time lag τ , the expectation is computed according to its definition, but also by averaging over all resource blocks for better statistics.

D. User Equipment

As mentioned at the beginning of Sec. II, each UE is a two-channel USRP, four of which were used in these measurements to provide a total of 8 spatial streams. The USRPs were mounted in carts to emulate pedestrian behaviour and in cars for higher levels of mobility, as shown in Fig. 2. Sleeve dipole antennas were used in each case. On the carts, the dipole antennas were attached directly to both RF chains of the USRP with vertical polarisation. With a fixed spacing of 2.6λ , these can either be considered as two devices in very close proximity or as a single, dual-antenna device. In Fig. 2, the USRPs shown in carts each have only one antenna connected. For the cars, the antennas were roof mounted with vertical polarization on either side of the car, giving a spacing of approximately 1.7 m. Each UE's RF chain operates with a different set of frequency-orthogonal pilots and synchronises over-the-air (OTA) with the BS using the primary synchronisation signal (PSS) broadcast at the start of each 10 ms frame. The PSS was transmitted using a static beam pattern and the local oscillators (LOs) of the UEs were global positioning system (GPS) disciplined to lower carrier frequency offset, thereby improving stability during the measurements.

III. MEASUREMENT SCENARIO

A mixture of both pedestrian and vehicular UEs were used so that it would be possible to observe how the massive MIMO channel behaves over time in a more dynamic situation. Each user transmitted with the same fixed power level and $\mathbf{Y}_r \forall r$



Fig. 3. Overview of the measurement scenario at the campus of the Faculty of Engineering (LTH), Lund University, Sweden. Arrows indicate the direction of movement for the cars C1 and C2. Pedestrians P1 and P2 moved within the zones indicated by their white boxes.

was captured for a 30 s period. Two pedestrian carts, indicated by P1 and P2, moved pseudo-randomly at walking pace to and from one another for the measurement duration, whilst two cars, shown as C1 and C2, followed the circular route shown. For the temporal results concerning the cars, it was ensured that the captures analysed were from a period of the scenario where the cars did not exceed our maximum $\lambda/2$ measurement speed of 29 km/h. Over the course of the entire capture, the cars completed approximately two laps and arrived back at the starting position indicated in Fig. 3. With the cars moving in this pattern, the devices are, on average, more distributed in the azimuth, but when C1 and C2 pass in parallel to the pedestrian carts they become more clustered in a perpendicular line to the BS.

IV. RESULTS

The temporal results were based on two different time periods within the 30 second mobility scenario. Channel hardening and power correlation results are presented first for one car user using a 3 second period of the full 30 second capture, specifically between 20.5 s and 23.5 s. Time correlation results are then shown for a 4 second period between 10 s and 14 s where both cars travel in parallel to the BS. For both of these time periods, the vehicle speed remains below 29 km/h.

A. Power Correlation

Fast-fading is shown to disappear theoretically when letting the number of BS antennas go to infinity, as discussed in [1] and [2]. Whilst the measured scenarios will have been more of a Rician than Rayleigh nature due to the UEs being predominantly in LOS, it was still possible to inspect the less severe fading dips of a single channel for a single UE

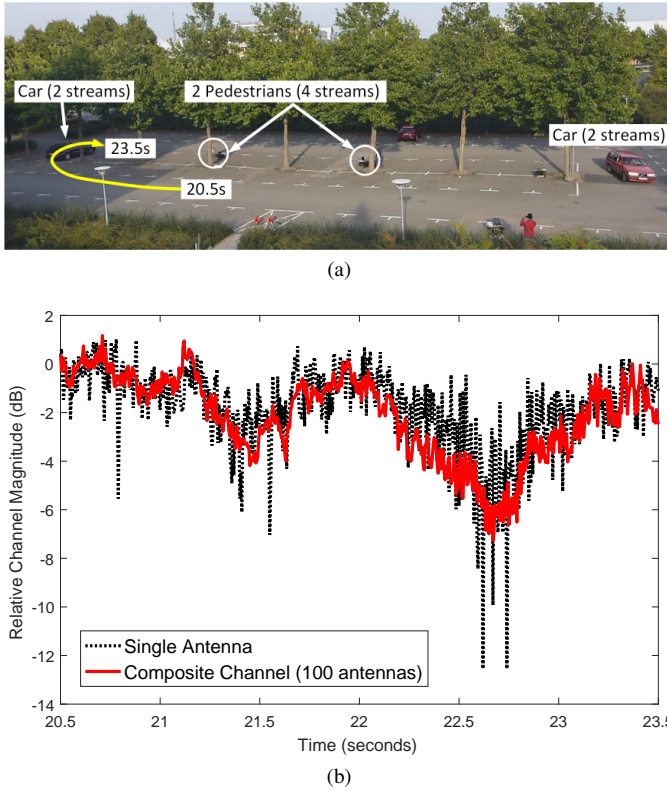


Fig. 4. Resilience to fading. a) View from BS with 3 second car-based user path indicated. b) Relative channel magnitude for both a single antenna and the composite MIMO channel to the depicted user over the 3 second period.

and evaluate them against the composite channel formed by the 100×8 massive MIMO system. In Fig. 4a, a 3 second portion of the captured mobile scenario is shown as viewed from the BS. An arrow indicates the movement of one of the cars during this three second period. For one UE in this car over the acquisition period shown, the channel magnitude of a single, vertically polarised BS antenna was extracted, along with the respective diagonal element of the user side Gram matrix $\mathbf{H}_r^H \mathbf{H}_r$ for one resource block r . Their magnitudes are plotted against each other in Fig. 4b after normalization. It can be seen that the composite channel tends to follow the average of the single antenna case, smoothing out the faster fading extremities, and larger variations occur over the course of seconds rather than milliseconds.

Fig. 5 shows the correlation of the signal power over time offset for a pedestrian UE and a car UE when using either one antenna or 100 antennas. Due to the channel hardening and the constructive combining of 100 signals, the power levels are much more stable as compared to the single antenna case. For this particular case, with 100 antennas, power control can be done at least five times slower than with a single antenna. These two figures show, that performance of this nature not only demonstrates an improvement in robustness and latency due to the mitigation of fast-fade error bursts, but also that it is possible to greatly relax the update rate of power control when combining signals from many antennas.

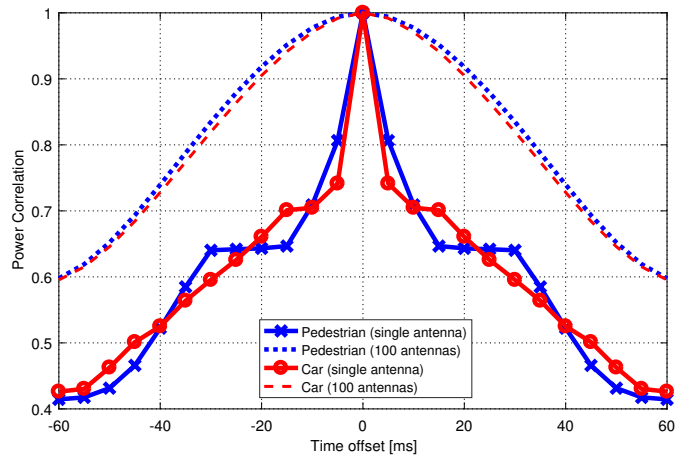


Fig. 5. Correlation of the power for signal on one antenna versus 100 antennas for a pedestrian and car UE.

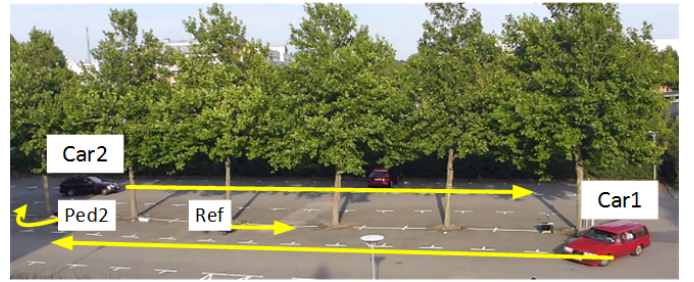


Fig. 6. 4 second subset of mobility scenario (10s to 14s of full 30 second capture) used for temporal analysis. Arrows indicate the movement of each UE over the 4 s duration. Car 2 does not exceed the maximum allowed speed of 29 km/h.

B. Channel Correlation

As a UE moves, it is of interest to view the correlation of the MIMO channel vectors over time in order to ascertain how quickly the channel becomes significantly different. This will play a part in determining the required channel estimation periodicity for a given level of performance. In Fig. 6, a 4 s second period of the 30 second mobility scenario is shown, with the arrows indicating the movement of each UE during that period. Using one UE from Car 2, the absolute values of the time correlation function for all resource blocks over the 4 second period are shown in Fig. 7 for the first 1.5 s of movement. Within the first 500 ms at this speed, the level of correlation has dropped significantly in the 100 antenna case to 0.3, whilst the 8 antenna case remains above 0.8 for the entire 1.5 s duration with a far shallower decay. For the 8 antenna and 100 antenna cases to become decorrelated by 20 percent, it takes 1455 ms and 205 ms respectively; a factor difference of approximately 7. This highlights how the precise spatial focusing of energy provided by massive MIMO translates to a larger decorrelation in time from far smaller movements in space. The acceptable level of decorrelation will depend upon many factors such as the desired level of performance, the

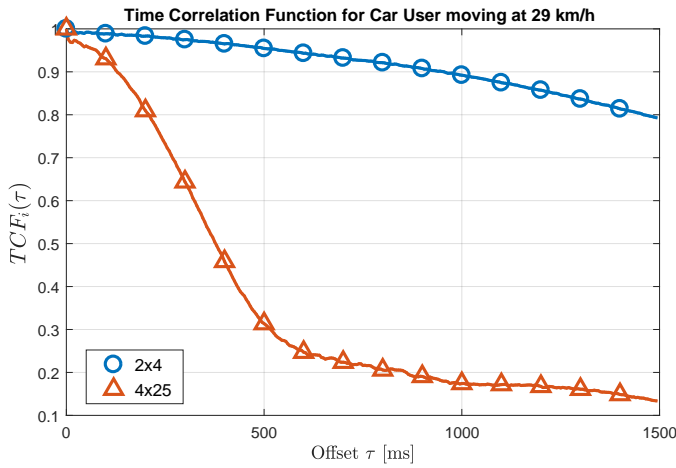


Fig. 7. Correlation of the composite channel over time for all resource blocks of car 2 at a speed of 29 km/h. 100 antenna and 8 antenna cases are shown in 4x25 and 2x4 configurations respectively. Both curves are normalized to themselves, so array gain is not visible here.

detection/precoding technique and the modulation and coding scheme (MCS), but this result provides some insight into how rapidly a real channel vector can change in massive MIMO under a moderate level of mobility when compared to a more conventional number of antennas.

V. CONCLUSIONS

The temporal performance of a 100×8 real-time massive MIMO system operating in a LOS scenario with moderate mobility has been presented. To the best of the authors' knowledge, these are the first results of their kind that begin to indicate the performance of massive MIMO as the composite channel changes over the course of a more dynamic scenario. When considering the correlation of mobile channel vectors over time, it was shown that the 100 antenna case decorrelated by 20% 7 times faster than the 8 antenna case, providing an indication of the spatial focusing effect in a MIMO system. In addition, the power correlation results indicate that power control algorithms may be able to operate 5 times slower than a single antenna case due to the channel hardening effect.

ACKNOWLEDGMENT

The authors wish to acknowledge and thank all academic staff and post graduate students involved who contributed to the measurement trial operations. They also acknowledge the financial support of the Engineering and Physical Sciences Research Council (EPSRC) Centre for Doctoral Training (CDT) in Communications (EP/I028153/1), the European Union Seventh Framework Programme (FP7/2007-2013) under grant agreement no. 619086 (MAMMOET), NEC, NI, the Swedish Foundation for Strategic Research and the Strategic Research Area ELLIIT.

REFERENCES

[1] T. L. Marzetta, "Noncooperative Cellular Wireless with Unlimited Numbers of Base Station Antennas," *IEEE Transactions on Wireless Communications*, vol. 9, no. 11, pp. 3590–3600, nov 2010.

[2] E. G. Larsson *et al.*, "Massive MIMO for next generation wireless systems," *IEEE Communications Magazine*, vol. 52, no. 2, pp. 186–195, February 2014.

[3] E. Björnson, J. Hoydis, M. Kountouris *et al.*, "Massive MIMO Systems With Non-Ideal Hardware: Energy Efficiency, Estimation, and Capacity Limits," *IEEE Transactions on Information Theory*, vol. 60, no. 11, pp. 7112–7139, Nov 2014.

[4] J. Hoydis *et al.*, "Massive MIMO in the UL/DL of Cellular Networks: How Many Antennas Do We Need?" *IEEE Journal on Selected Areas in Communications*, vol. 31, no. 2, pp. 160–171, feb 2013.

[5] C. Shepard *et al.*, "Argos: practical many-antenna base stations," in *Proceedings of the 18th annual international conference on Mobile computing and networking - Mobicom '12*, no. i. ACM Press, 2012, p. 53.

[6] C. Shepard *et al.*, "ArgosV2 : A Flexible Many-Antenna Research Platform," Tech. Rep., 2013.

[7] H. e. a. Suzuki, "Highly spectrally efficient Ngara Rural Wireless Broadband Access Demonstrator," in *2012 International Symposium on Communications and Information Technologies, ISCIT 2012*, 2012, pp. 914–919.

[8] Y. Li, Y. Xm, M. Dong *et al.*, "Implementation of full-dimensional MIMO (FD-MIMO) in LTE," in *2013 Asilomar Conference on Signals, Systems and Computers*, Nov 2013, pp. 998–1003.

[9] Y. H. Nam, B. L. Ng, K. Sayana *et al.*, "Full-dimension MIMO (FD-MIMO) for next generation cellular technology," *IEEE Communications Magazine*, vol. 51, no. 6, pp. 172–179, June 2013.

[10] W. Zhang *et al.*, "Field Trial and Future Enhancements for TDD Massive MIMO Networks," vol. 7, pp. 2339–2343, 2015.

[11] "Facebook Project Aries," 2016. [Online]. Available: <https://code.facebook.com/posts/1072680049445290/introducing-facebook-s-new-terrestrial-connectivity-systems-terragraph-and-project-ar>

[12] J. Vieira *et al.*, "A flexible 100-antenna testbed for Massive MIMO," in *Globecom Workshops (GC Wkshps)*, 2014, pp. 287–293.

[13] S. Malkowsky, J. Vieira, L. Liu *et al.*, "The World's First Real-Time Testbed for Massive MIMO: Design, Implementation, and Validation," *IEEE Access*, submitted, 2016. [Online]. Available: <https://arxiv.org/pdf/1701.01161.pdf>

[14] P. Harris *et al.*, "LOS Throughput Measurements in Real-Time with a 128-Antenna Massive MIMO Testbed," in *Globecom*, 2016, in press.

[15] P. Harris, W. B. Hasan, S. Malkowsky *et al.*, "Serving 22 Users in Real-Time with a 128-Antenna Massive MIMO Testbed," in *2016 IEEE International Workshop on Signal Processing Systems (SiPS)*, Oct 2016, pp. 266–272.

[16] P. Kela, X. Gelabert, J. Turkka *et al.*, "Supporting mobility in 5G: A comparison between massive MIMO and continuous ultra dense networks," in *2016 IEEE International Conference on Communications (ICC)*, May 2016, pp. 1–6.

[17] A. Papazafeiropoulos, H. Ngo, and T. Ratnarajah, "Performance of Massive MIMO Uplink with Zero-Forcing receivers under Delayed Channels," *IEEE Transactions on Vehicular Technology*, vol. PP, no. 99, pp. 1–1, 2016.

[18] A. Papazafeiropoulos, "Impact of General Channel Aging Conditions on the Downlink Performance of Massive MIMO," *IEEE Transactions on Vehicular Technology*, vol. PP, no. 99, pp. 1–1, 2016.

[19] "USRP-RIO 2943 Datasheet," 2014. [Online]. Available: <http://www.ni.com/datasheet/pdf/en/ds-538>

[20] J. Vieira, F. Rusek, O. Edfors *et al.*, "Reciprocity Calibration for Massive MIMO: Proposal, Modeling and Validation," *CoRR*, vol. abs/1606.05156, 2016. [Online]. Available: <http://arxiv.org/abs/1606.05156>

[21] S. Malkowsky, J. Vieira, K. Nieman *et al.*, "Implementation of Low-Latency Signal Processing and Data Shuffling for TDD Massive MIMO Systems," in *2016 IEEE International Workshop on Signal Processing Systems (SiPS)*, Oct 2016, pp. 260–265.

[22] A. Molisch, *Wireless Communications*, ser. Wiley - IEEE. Wiley, 2010. [Online]. Available: <https://books.google.co.uk/books?id=vASyH5-jfMYC>